A Wide-band Hybrid Antenna for Use in Reverberation Chambers

Andrew C Marvin *Fellow IEEE*, Giuseppe Esposito, John F Dawson *Member IEEE*,
Ian D Flintoft *Member IEEE*, Linda Dawson, Jeremy A K Everard & Gregory C R Melia
Dept. of Electronics, University of York
York, UK
andy.marvin john.dawson ian.flintoft l.dawson jeremy.everard gcrm100 @york.ac.uk

***Abstract*—This paper describes the design and performance of a wide-band hybrid antenna suitable for use in reverberation chambers. The antenna is characterised over the frequency range 100 MHz to 25 GHz showing that it performs well above 200 MHz although its ultimate highest operating frequency has not been established.**

***Index Terms*—Hybrid Antennas, Reverberation Chambers**

I. Introduction

In most cases the antennas used in reverberation chambers are of types that were originally designed for other test environments or other applications. In particular, the radiation pattern of an antenna used in a reverberation chamber is of less importance, since in a well stirred chamber the average antenna pattern tends to isotropic and the vector averaged input reflection coefficient is identical to the free-space value. We therefore consider the ideal antenna to be one with a compact form-factor, which has a low reflection coefficient whilst operating over the full frequency range of a typical chamber.

In this paper we describe a hybrid antenna that operates in the frequency range from 200 MHz to 25 GHz as defined by the magnitude of its input reflection coefficient (S11) being less than 0.316 (-10 dB). The antenna is designed to exhibit high efficiency and can be operated mounted either within the working volume of the chamber or as a wall mounted antenna.

The antenna is a hybrid structure operating at lower frequencies as a broadband monopole and at higher frequencies as an exponential taper or Vivaldi antenna (*Vivaldi antenna – a name inspired by the cross-section of a Baroque trumpet and given to the antenna by its inventor Peter Gibson, a keen amateur musician, on the 300th anniversary of the composer Vivaldi's birth in 1978*) [1]. The overall dimensions of the antenna described here are 375 mm by 300 mm by 300 mm (LxWxH). The structure could be scaled to accommodate different frequency ranges.

The wideband performance of the antenna ensures that all the advantages associated with such performance, the decrease in test time associated with no antenna changes and the associated improvements to cable and connector reliability, are available.

In this paper we present a description of the basic antenna structure along with data illustrating its measured and modelled performance both inside and outside a reverberation chamber.

An image of the hybrid antenna structure is shown in Fig. 1. The ground-plane has dimensions of 375 mm by 300 mm. The hybrid monopole-Vivaldi structure has a height of 302 mm and a total width of 250 mm. It is fabricated from 600 μm thick brass sheet. This is fed against the ground-plane through a 50 Ω SMA receptacle visible at the left-hand side of the ground-plane. In order to achieve maximum operating bandwidth and efficiency, the antenna has no balun. The exponential taper on the monopole-Vivaldi structure is a simple exponential of the form:

$$y = a\mathrm{e}^{bx}. \quad (1)$$

Here the scale constants a and b are chosen such that the height, y, is 1 mm where x is zero and y is 300 mm where x is 250 mm. The circular curve of radius 500 mm starting 20 mm directly above the feed point, with a chord of 262 mm shown in Fig. 1 is chosen to increase the electrical length of the antenna in its low frequency monopole mode in order to improve the input reflection coefficient at 200 MHz. The top corners are rounded with a 20 mm radius which exactly meets the end of the circular curve on the back edge and intersects the exponential on the front edge.

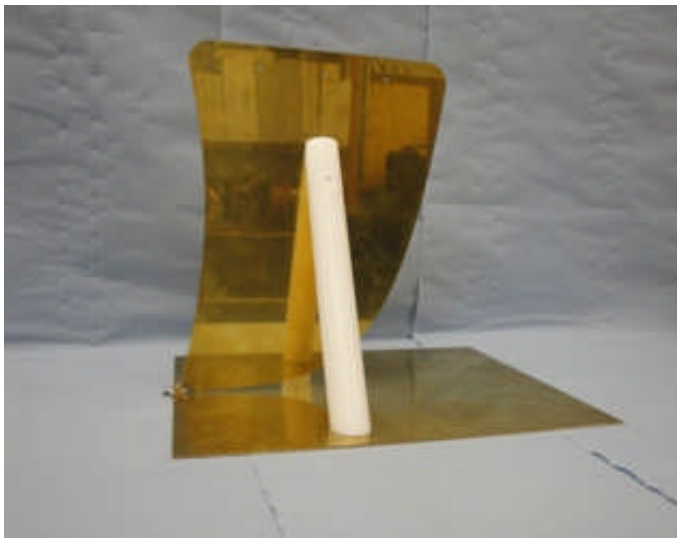

Fig.1. Photograph of the hybrid antenna structure.

The dielectric supports of the monopole-Vivaldi structure are made from 30 mm diameter PTFE rod and are placed away from the Vivaldi taper to minimise dielectric loss. Fig. 2 shows a close-up view of the feed point of the antenna with the SMA receptacle mounted in the feed block which has a 5 mm square cross-section.

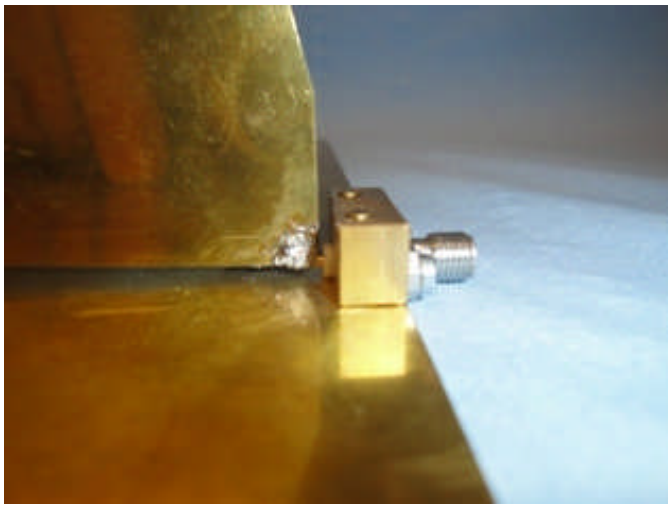

Fig. 2. Close-up view of the antenna feed.

.

II. A NUMERICAL MODEL OF THE ANTENNA

In order to verify the operation of the antenna and to allow for subsequent optimization a method-of-moments (MoM) model using the CONCEPT program has been used to examine the surface currents on the antenna and to predict the input reflection coefficient [2].

The structure was modelled using an unstructured quadrilateral mesh generated by the Gmsh program [3]. The global segmentation size was set at about 20 mm in order to produce a mesh that was valid to 2 GHz. The segmentation size around the feed point and edge of the exponential taper was about 1 mm in order to model the rapid current gradients at these locations. The coaxial feed was modelled using a short wire between the end of the taper on the vertical plate and a small closed metallic block representing the SMA connector and its housing. A 50 Ω impedance voltage source was impressed on the end of the source wire adjacent to the block. Convergence of the mesh was verified by reducing both global segmentation size and that near the feed wire.

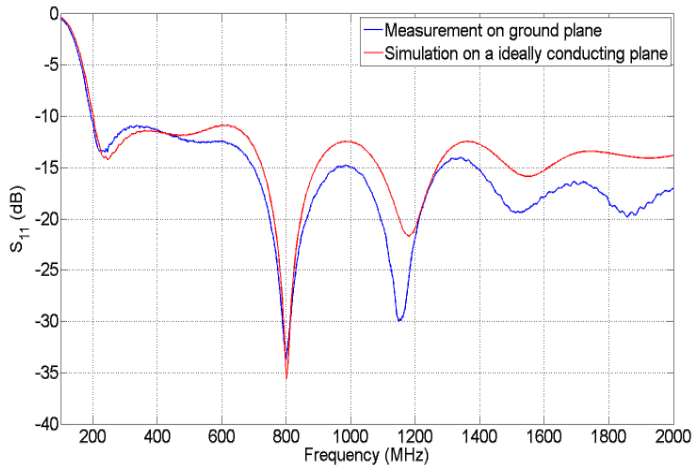

Fig. 3. Comparison of measured and modelled input reflection coefficient (S11).

The input reflection coefficient predicted by the model compared to the measured value, in the frequency range from 100 MHz to 2 GHz, is shown in Fig. 3. The antenna was placed on an extended metal ground-plane on an open-area test site (OATS) for this measurement. It is clear from Fig.3 that the model accurately captures the measured antenna input reflection coefficient.

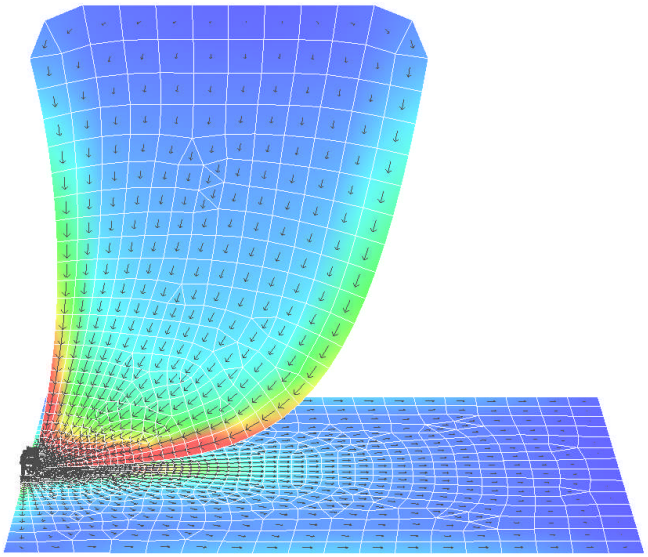

Fig. 4. Current distribution at 200 MHz.

Fig. 4 shows the computed current distribution on the antenna at 200 MHz. Here the monopole-Vivaldi structure is operating in its monopole mode. The current density reduces towards the top of the structure and all the phase indicating arrows are in the same direction. Significant current flows up each edge of the structure. Note that in this and subsequent diagrams the colour is indicative of the current density with the spectrum going from red (high) to blue (low). In Fig. 5 the current density around the feed block is shown. The source wire is shown in blue.

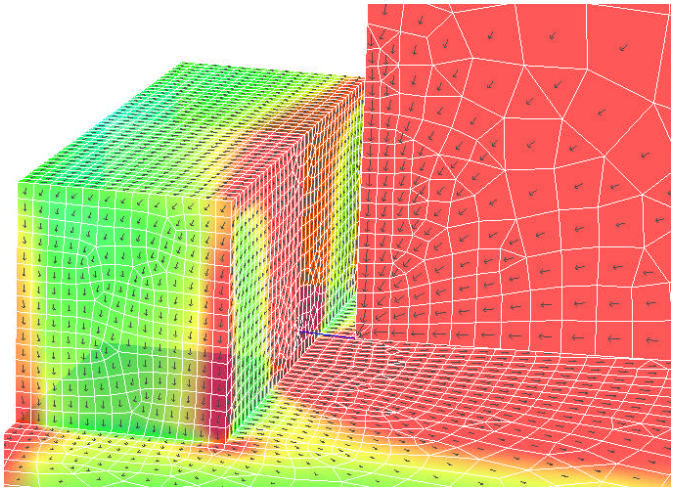

Fig.5. Detail of the current distribution at 200 MHz over the feed block.

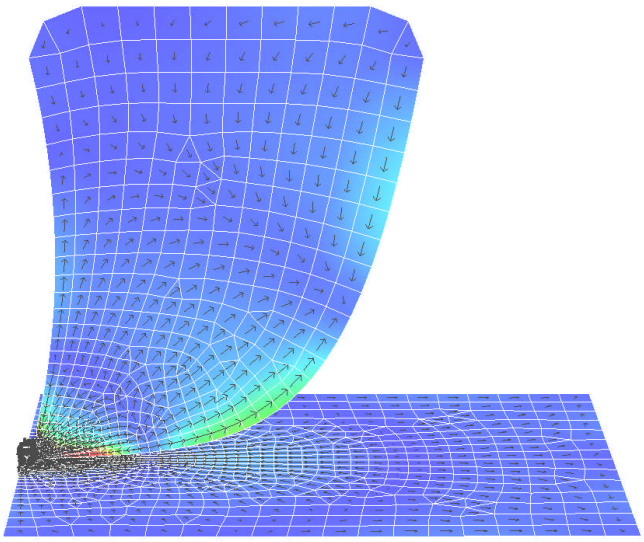

Fig. 6. Current distribution at 1 GHz.

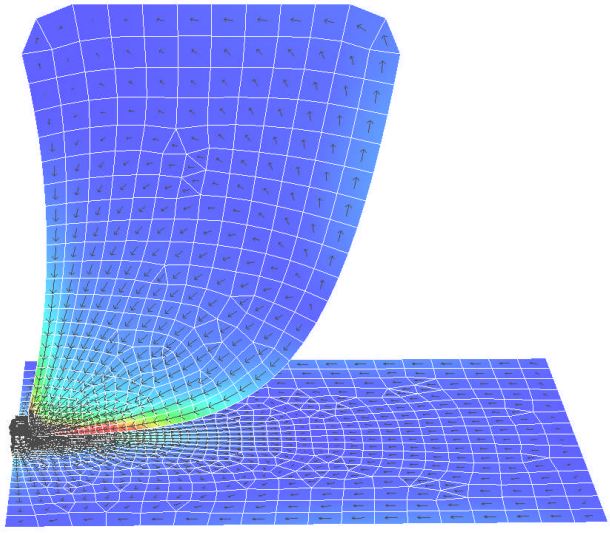

Fig. 7. Current distribution at 400 MHz.

Fig. 6 shows the current distribution at 1 GHz. Here it can be observed that the current is crowded towards the exponential edge of the structure indicating that the antenna is operating in its Vivaldi mode. The phase indicating arrows show regions of phase reversal as would be expected in this mode.

The transition region between the two modes appears well controlled. The key to it is the dominant operation of the Vivaldi mode at the frequency where the monopole would become a half-wave in length. The left-hand edge of the structure shown in the preceding figures has been lengthened by incorporating the curve in order to increase the structure's length. From Fig. 3 it can be seen that the quarter-wave resonance in the monopole mode is at 250 MHz, indicating a half-wave response at 500 MHz.

Examination of Fig. 7 showing the current distribution at 400 MHz demonstrates that the Vivaldi mode has become established at this frequency, significantly below the half-wave monopole frequency.

III. MEASUREMENTS OF THE ANTENNA'S PERFORMANCE

Fig. 8 is an image of the antenna undergoing free-space measurements on the OATS. It is placed on an 800 mm polystyrene block above outdoor pyramidal absorbers. Note the inclusion of the ferrite choke on the feed cable. The graph in Fig. 9 shows input reflection coefficient measurements (S11) from 100 MHz to 6 GHz with the choke at three different positions on the cable and with no choke present. These data indicate that the lack of a balun is not significant when the antenna is operated in this manner. Modelling results indicated that the fraction of the total feed current present on the feed cable is typically less than 10 % of the total, with the antenna in free space, which we expect to be the worst-case condition.

Fig. 8. Free space measurement on an OATS.

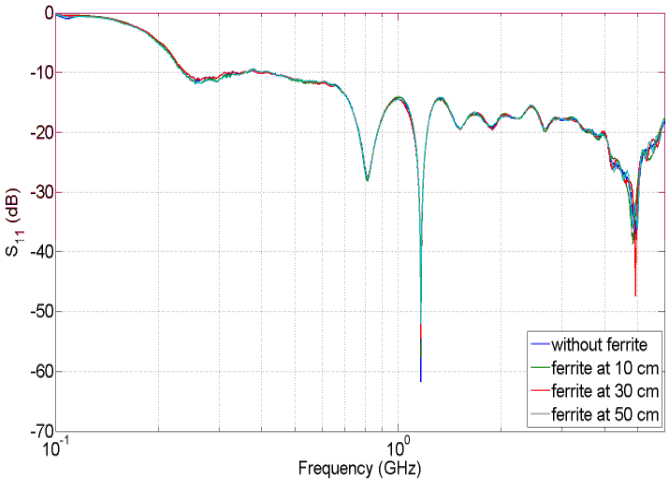

Fig.9. Free space reflection coefficients of the antenna with and without ferrite chokes on the feed cable.

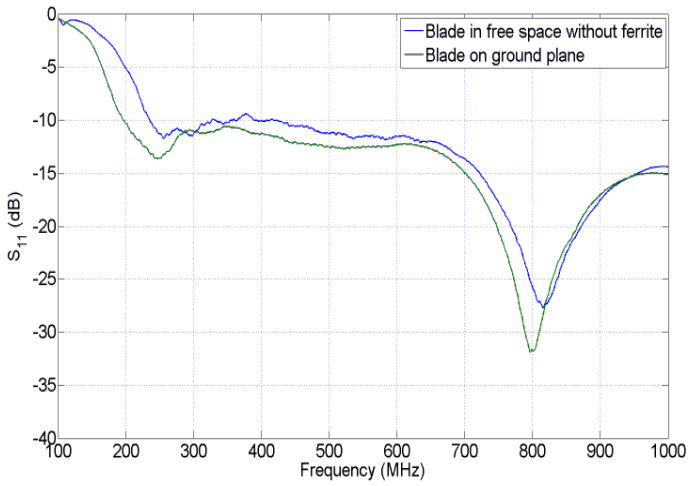

Fig. 10. Input reflection coefficient (S11) of the antenna up to 1 GHz

.

Fig. 10 shows a comparison of the measured input reflection coefficient in the frequency range from 100 MHz to 1 GHz with the antenna in free-space and placed on the OATS ground-plane. It can be seen that the target reflection coefficient is met from 200 MHz on the ground-plane whilst a usable reflection coefficient (S11 of -5 dB) is obtained at 200 MHz when the antenna is operated in free-space.

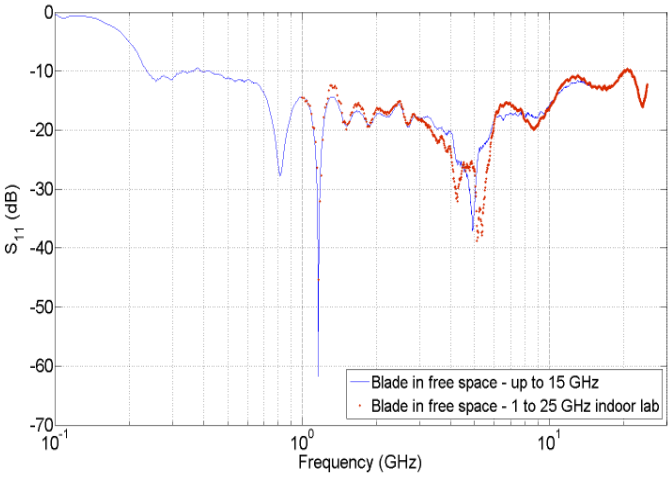

Fig. 11. Free-space reflection coefficient (S11) of the antenna from 100 MHz to 25 GHz.

The data from 1 GHz to 15 GHz are similar in both free-space and on the ground-plane. The full frequency range of the antenna can be seen in Fig. 11. These data show the free-space reflection coefficient from 100 MHz to 25 GHz. The measurements from 1 GHz to 25 GHz were made in an indoor laboratory where the higher frequency network analyser was situated. The antenna was hooded with absorber.

The agreement between the outdoor free-space measurement and the indoor free-space measurement is acceptable and the performance of the antenna is maintained to 25 GHz (S11 < 0.316, -10 dB).

IV. REVERBERATION CHAMBER MEASUREMENTS

Fig. 12 (upper) shows the antenna mounted on polystyrene in a reverberation chamber whilst Fig. 12 (lower) shows it on the floor of the chamber. The reverberation chamber has dimensions 4.8 m × 3.3 m × 2.2 m. The chamber has been demonstrated to have a lowest usable frequency of 200 MHz according to the field uniformity criteria detailed in IEC61000-4-21.

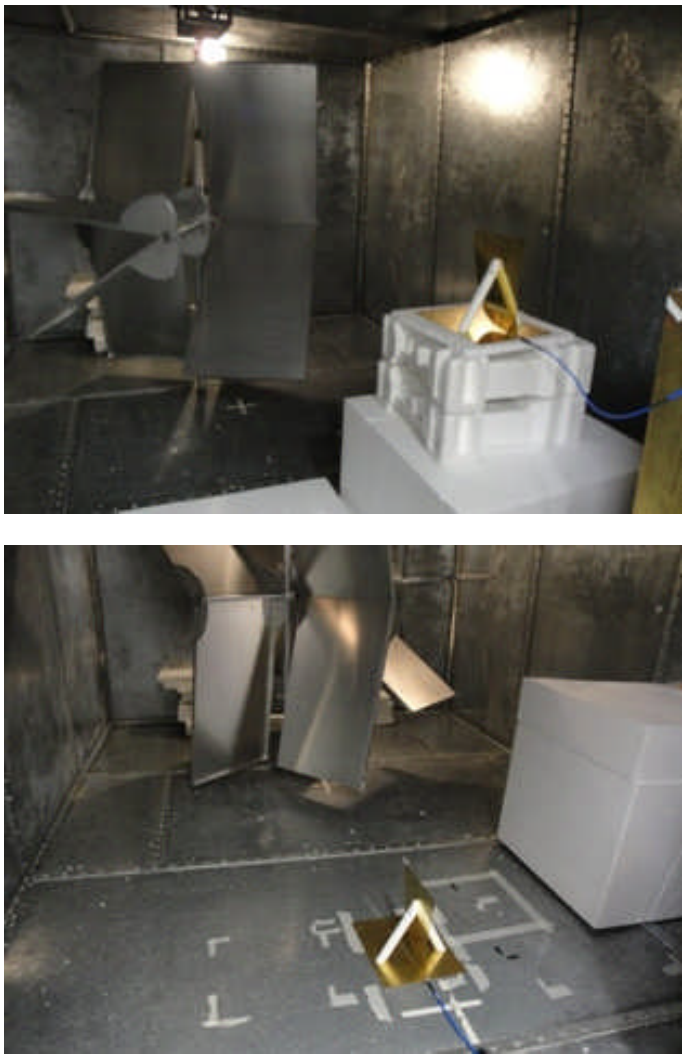

Fig. 12. The antenna in the reverberation chamber. In the top photograph the antenna is mounted well clear of the chamber wall while in the bottom photograph it is in contact with the floor.

Input reflection coefficient measurements were made with the antenna in these two locations. The vector average of these measurements over a complete stirrer rotation with 200 stirrer positions was taken and then over a frequency window of 50 MHz (100 data points) to further reduce the statistical variation.

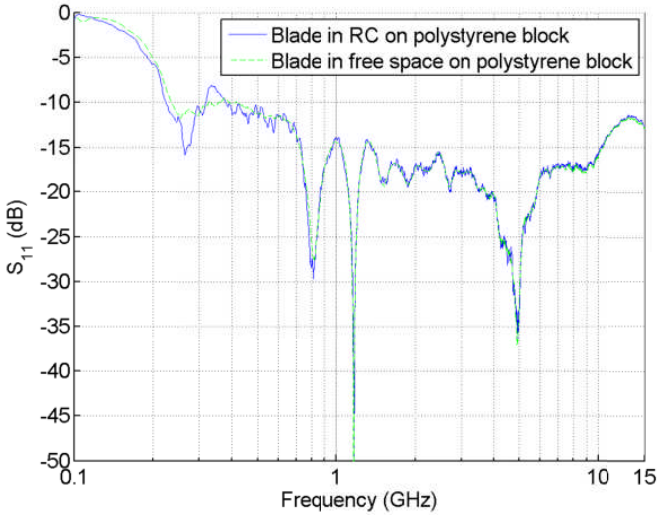

Fig. 13. Comparison of input reflection coefficients for free-space mode.

Fig. 13 shows the comparison of the free-space input reflection coefficient measurements taken on the OATS and the vector average values taken with the antenna in the reverberation chamber as in Fig. 12 (upper).

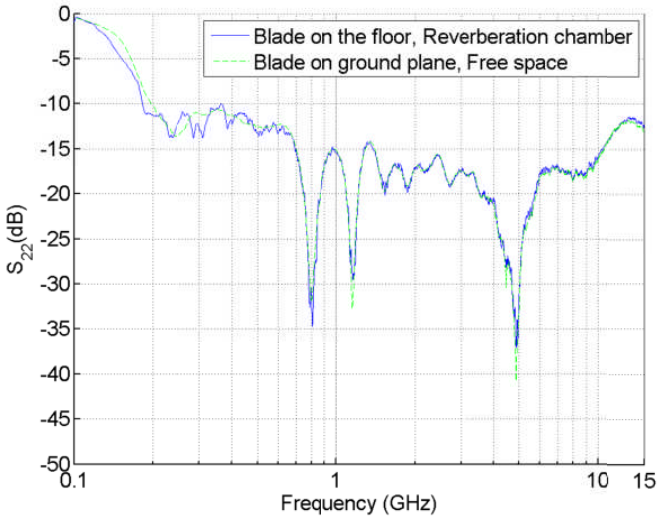

Fig.14. Comparison of input reflection coefficients for ground-plane mode.

Fig. 14 shows comparable data for the antenna operated in the ground-plane mode both on the OATS and in the reverberation chamber. In both Fig. 13 and Fig. 14 there is good agreement between the two measurement environments. This is to be expected as the vector average of the input reflection coefficient in the chamber over one stirrer rotation should be identical to the free-space input reflection coefficient [4].

The moving average function used in the frequency domain reduces the number of points it uses, linearly, towards the ends of the data-set so no averaging occurs at 100 MHz and 15 GHz. At 100 MHz the antenna reflection coefficient is large so this is of little consequence. At 15 GHz the average produced by the 200 stirrer positions is adequate so again the consequence is minimal. The largest difference between the reverberation chamber and free space results occurs between 200 and 400 MHz where the number of independent stirrer positions is expected to be small.

V. CONCLUSIONS

In this paper we have described the structure and performance of a new class of hybrid antenna specifically designed to offer wideband performance, with a low reflection coefficient, in a reverberation chamber, where the shape of the radiation pattern is not important. The antenna structure is such that it should offer a high level of efficiency as care has been taken to ensure that no dielectric material is present in areas where electric fields are at their maximum and no balun is used. The performance of the antenna has been demonstrated both by measurement in a reverberation chamber and in free-space over the frequency range from 200 MHz to 25 GHz and as such the antenna potentially replaces three existing antennas in this application, i.e. a biconical dipole, a log-periodic dipole array and a ridged waveguide horn. The antenna has been shown to operate in two modes. The first is as a broadband monopole from 200 MHz to around 400 MHz. The second is as a Vivaldi style structure from around 400 MHz to 25 GHz. Modelling the antenna using CONCEPT has demonstrated the two mode operation. We are currently undertaking optimisation of the antenna structure to further improve its performance and efficiency measurements are as yet incomplete. The current SMA connector feed has been used to allow us to explore the high frequency performance, whilst a larger diameter connector could be used if higher power capability is required.

VI. ACKNOWLEDGMENT

We gratefully acknowledge the assistance of Pratik Deshpande with measurements and the work carried out by students Peter Ludlow and Robert Salmon of the Department of Physics, University of York whose work on earlier Vivaldi antennas provided insight into the new design.

VII. REFERENCES

[1] P. J. Gibson “The Vivaldi aerial”, 9th European Microwave Conference, Brighton, UK, 17-20 Sept. 1979, pp.101-105.

[2] Technical University of Hamburg-Harburg, CONCEPT-II [Online] http://www.tet.tu-harburg.de/concept/index.en.html.

[3] C. Geuzaine and J.-F. Remacle, “Gmsh: a three-dimensional finite element mesh generator with built-in pre- and post-processing facilities”, International Journal for Numerical Methods in Engineering, vol. 79, no. 11, pp. 1309-1331, 2009.

[4] J. Ladbury, G. Koepke, D.Camell, “Evaluation of the NASA Langley Research Center Mode-Stirred Chamber Facility”, NIST Technical Note, no. 1508. January, 1999.

Marvin, A.; Esposito, G.; Dawson, J.; Flintoft, I.; Dawson, L.; Everard, J. & Melia, G. , "A wide-band hybrid antenna for use in reverberation chambers" , Electromagnetic Compatibility (EMC), 2013 IEEE International Symposium on , 222-226 , August, 2013 , DOI: 10.1109/ISEMC.2013.6670413